UNIVERSITY OF PARDUBICE

FACULTY OF CHEMICAL TECHNOLOGY

Department of General and Inorganic Chemistry

Yaraslava Milasheuskaya

Preparation of Novel N,N-Chelating Ligands and Their Application in Non-Transition Metal Chemistry

Theses of the Doctoral Dissertation

Pardubice 2025

Study program: **Inorganic Chemistry**

Study field: **Organometallic chemistry**

Author: **Yaraslava Milasheuskaya**

Supervisor: **prof. Ing. Roman Jambor, Ph.D.**

Year of the defence: 2025

References

MILASHEUSKAYA, Yaraslava. *Preparation of Novel N,N-Chelating Ligands and Their Application in Non-Transition Metal Chemistry.* Pardubice, 2025. 161 pages. Dissertation thesis (Ph.D.). University of Pardubice, Faculty of Chemical Technology, Department of General and Inorganic Chemistry. Supervisor Prof. Ing. Roman Jambor, Ph.D.

Abstract

This dissertation investigates the synthesis, modification, and reactivity of N,N-chelating ligands featuring oxygen and nitrogen donor atoms within the structure of an asymmetric 2,6-pyridine framework. This work investigated the influence of substituents on the coordination and reactivity properties of N,N,PO ligands with salts of non-transition metals. In particular, the utilisation of these ligands for the stabilisation of organometallic complexes and their potential in the low-temperature synthesis of GeTe nanoparticles were studied. Additionally, the research explores the catalytic applications of selected complexes in the polymerisation of cyclic esters (ROP) and their potential for synthesising star-shaped polyesters.

Keywords

N,N-chelating ligands, non-transition metals, GeTe nanoparticle synthesis, catalysis of polymerisation reactions (ROP)

Abstrakt

Tato disertační práce se zaměřuje na syntézu, modifikaci a reaktivitu N,N-chelatujících ligandů obsahujících donorové atomy kyslíku a dusíku ve struktuře asymetrického 2,6-pyridinového skeletu. Práce se věnuje studiu vlivu substituentů na koordinační schopnosti N,N,PO ligandů, reaktivitě s různými solemi nepřechodných prvků. Zvláštní pozornost byla věnována využití ligandů pro stabilizaci organokovových komplexů a jejich potenciálu v nízkoteplotní syntéze nanočástic GeTe. Práce rovněž obsahuje výzkum katalytického využití vybraných komplexů v polymerizačních reakcích cyklických esterů (ROP) a možnosti syntézy hvězdicových polyesterů.

Klíčová slova

N,N-chelatující ligandy, nepřechodné prvky, syntéza GeTe nanočástic, katalýza polymerizačních reakcí (ROP)

Table of Contents

1. Introduction

The continuous development of synthetic methods and the search for new chemical and physical properties to enable the creation of specialized metal complexes have made ligand design a critical part of synthetic organic chemistry. The importance of this area of research extends beyond catalytic chemistry[1]. It includes the development of porous and functional supramolecular materials[2], as well as the preparation of complexes capable of activating small molecules[3]. N,N-chelating ligands are one of the most widely used ligands in coordination chemistry, not only for transition metals[4] but also for non-transition elements[5].

N,N-chelating ligands can be generally divided into two structural types:

1) ligands with an aliphatic backbone, where the key motif consists of two nitrogen atoms connected by a carbon linker (amidines, diazabutadienes (DAB), β-diketimines (BDI)) (Figure 1a);
2) ligands with an aromatic backbone, where at least one of the nitrogen atoms is part of an aromatic ring (polypyridyl ligands (Bpy, Tpy) and pyridine diimines (DIMPY)) (Figure 1b).

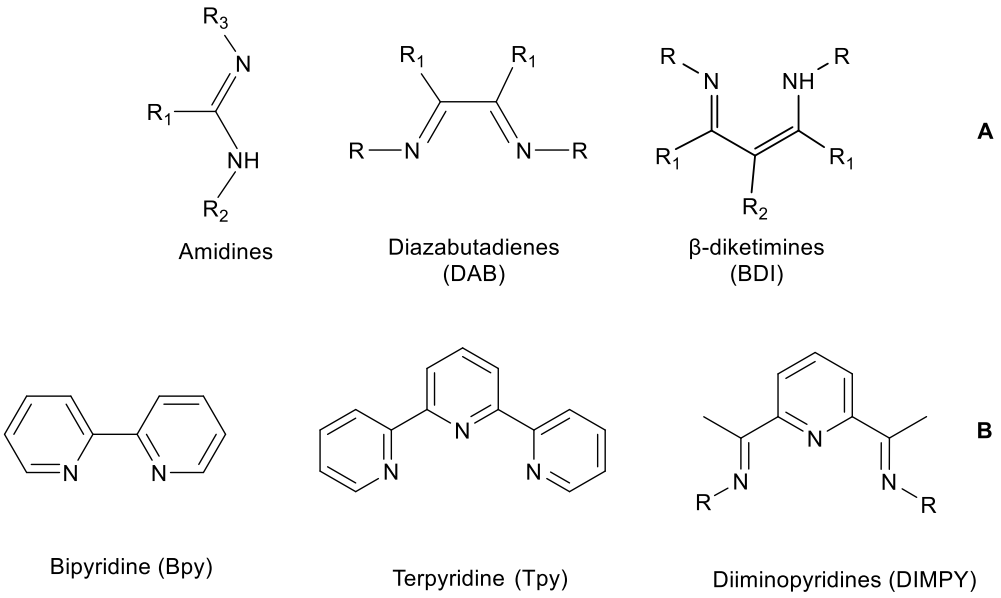

Figure 1: a) N,N-chelating ligands with an aliphatic backbone, b) N,N-chelating ligands with an aromatic backbone.

The noticeable trend in the synthesis of symmetrical ligands comes from the fact that it is generally less challenging than their unsymmetrical counterparts.[6] The introduction of functional groups into the organic backbone of the precursor occurs by carrying out the appropriate reaction steps in double the amount compared to the starting organic precursor. The resulting ligands have predictable reactivity with p-block elements, and due to their lower variability, they are often used to study the influence of side alkyl or aryl groups on the reactivity and structure of organometallic complexes.[7] These ligands are encountered much more frequently in the literature than unsymmetrical N,N-coordinating ligands. Particularly advantageous is the introduction of a different donor atom that has different interaction capabilities compared to nitrogen. The preparation of

such ligands requires multi-step reactions and more advanced techniques, which results in reduced yields or the need to introduce protection groups.[8] Different donor atoms in the ligand backbone allow the preparation of organometallic complexes where the ligand is bound to the central atom in various ways, depending on its nature, and where greater stabilisation of the central atom can occur.

Transition metal complexes based on N,N-chelating ligands are well-studied, with some complexes already being used as catalysts for a long time. However, in recent decades, attention has shifted to the chemistry of these ligands with non-transition elements due to their abundance in the Earth's crust, and attempts to optimize well-known reaction pathways with greener approaches.[9] Organometallic compounds of non-transition elements are traditionally associated with synthetic and handling issues, which, compared to transition metal complexes, results in their limited number and actual applicability. However, arming N,N-chelating ligands with bulkier substituents such as biphenyl (Bph), 2,6-Diisopropylphenyl (Dipp), 2,6-Dimethylphenyl (Dmp), Di-tert-buthylphenyl (Dtp) (Figure 2) have enabled the preparation several of neutral[10] and ionic[11] complexes of p-block elements in consistently high yields.

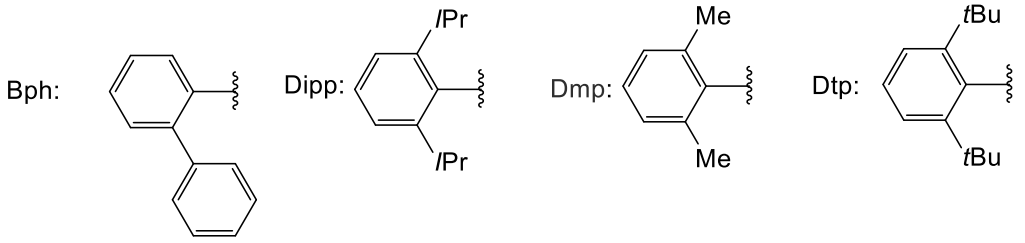

Figure 2: Typical bulky substituents in N,N-chelating ligands used for stabilizing non-transition complexes.

2. Objectives

The aim of this work was to expand the knowledge on the preparation and reactivity of unsymmetrical N,N,PO ligands, which, in terms of their structure, resemble the symmetrical N,N,N-chelating diiminopyridine DIMPY ligands. This type of unsymmetrical N,N,PO-chelating ligand is based on a 2,6-pyridine backbone, where one *ortho*-position contains a nitrogen atom in the form of a traditional imine fragment C=N, while in the second *ortho*-position, an $R_2R_3P(O)$ group is located, available for P(*O*)→E coordination. The foundation of this study was laid in the master's thesis by M. Syková[12], where ligands **L¹** and **L²** (Figure 3) were prepared, and their reactivity with $GeCl_2$ and $SnCl_2$ was investigated.

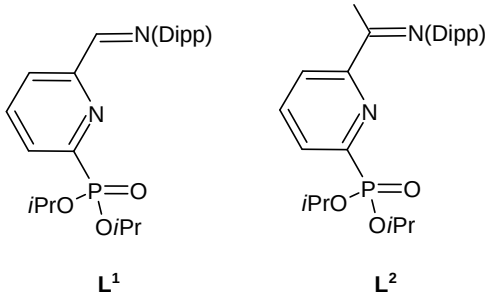

Figure 3: NNPO-chelating ligands known from the literature.

The following objectives were set as a research scope for this dissertation:

1) Modification of the ligand backbone and investigation of the influence of groups other than O*i*Pr on the P(O) fragment on the resulting products in the synthesis of tin complexes.
2) Expansion of the reactivity of N,N,PO-type ligands to other non-transition elements.
3) Testing the stability of the prepared organometallic complexes and exploring their further reactivity in the case study of their reduction.
4) Investigation of the potential use of stable complexes in catalysis and materials chemistry.

3. Results and Discussion

1.1 Synthesis of starting ligands L^{3-6}

The synthesis was carried out via a C–P cross-coupling reaction between the corresponding precursor 2-[CR=N(Dipp)]-6-Br-C_5H_3N (**$L^{3,5}$:** R = H, **$L^{4,6}$:** R = CH_3) and correspondingly ethylphenylphosphinate (**L^{3-4}**) or diphenylphosphine oxide (**L^{5-6}**) in the presence of triethylamine. The reaction was catalyzed by a combination of 1,1`-bis(diphenylphosphino)ferrocene and palladium acetate as a catalyst (Scheme 1).

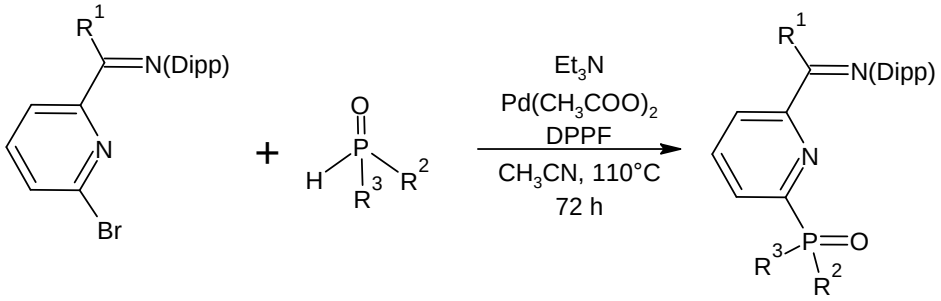

L^{3-6}

L^3: R^1 = H, R^2 = OEt, R^3 = Ph
L^4: R^1 = CH_3, R^2 = OEt, R^3 = Ph
L^5: R^1 = H, R^2 = R^3 = Ph
L^6: R^1 = CH_3, R^2 = R^3 = Ph

Scheme 1: Synthesis of unsymmetrical NNPO ligands $L^{3–6}$.

1.2 Reactivity of ligands L^{3-6} with $SnCl_2$

Based on previous findings made in our group about the capability of ligands **L^{1-2}** to react with $SnCl_2$ to form the complex compounds $[(L^{1-2})SnCl]^+[SnCl_3]^-$,[12] the newly prepared ligands **L^{3-6}** were subjected to an analogous reaction. The reaction afforded the corresponding ionic complexes $[(L^3)SnCl]^+[SnCl_3]^-$ (**1**), $[(L^4)SnCl]^+[SnCl_3]^-$ (**2**), $[(L^5)SnCl]^+[SnCl_3]^-$ (**3**) and $[(L^6)SnCl]^+[SnCl_3]^-$ (**4**) (Scheme 2). These results confirmed that ligands **L^{3-6}** can promote the auto-ionisation reaction of $SnCl_2$ in a manner analogous to that of ligands **L^{1-2}**.

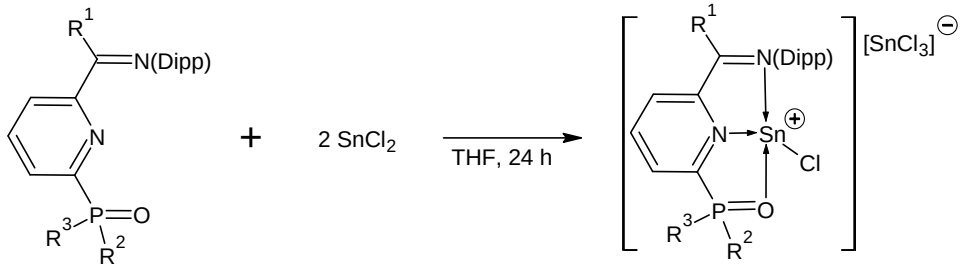

L$^{3-6}$ **1-4**

1: R^1 = H, R^2 = OEt, R^3 = Ph
2: R^1 = CH_3, R^2 = OEt, R^3 = Ph
3: R^1 = H, R^2 = R^3 = Ph
4: R^1 = CH_3, R^2 = R^3 = Ph

*Scheme 2: Synthesis of ionic tin(II) complexes **1–4**.*

In contrast, it has also been reported in the literature that N,N-chelating ligands bearing sterically demanding aryl groups in the *ortho*-position of the pyridine fragment exhibit different reactivity. In these cases, the formation of neutral complexes of the type [L→$SnCl_2$] was observed (Scheme 3).[13]

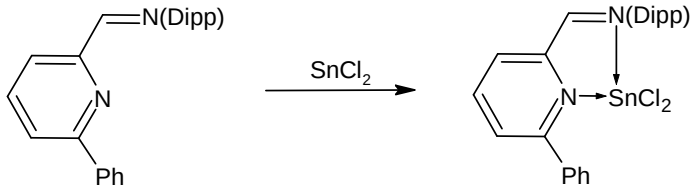

Scheme 3: Representative example of the reaction of an N,N-chelating ligand with $SnCl_2$ affording a neutral complex of the type [L→$SnCl_2$].

It is thus evident that the introduction of R_2P=O functional groups into the *ortho*-position of the iminopyridine ligands plays a crucial role in promoting the auto-ionisation reaction of $SnCl_2$.

Single-crystal X-ray diffraction analysis of complexes **1-4** unambiguously confirmed the presence of two oppositely charged species (cation [(**L**$^{3-6}$)SnCl]$^+$ and anion [$SnCl_3$]$^-$) within a single crystal unit. The molecular structures of compounds **1,** **2**·CH_2Cl_2, **3** a **4**·CH_2Cl_2 are depicted in Figure 4.

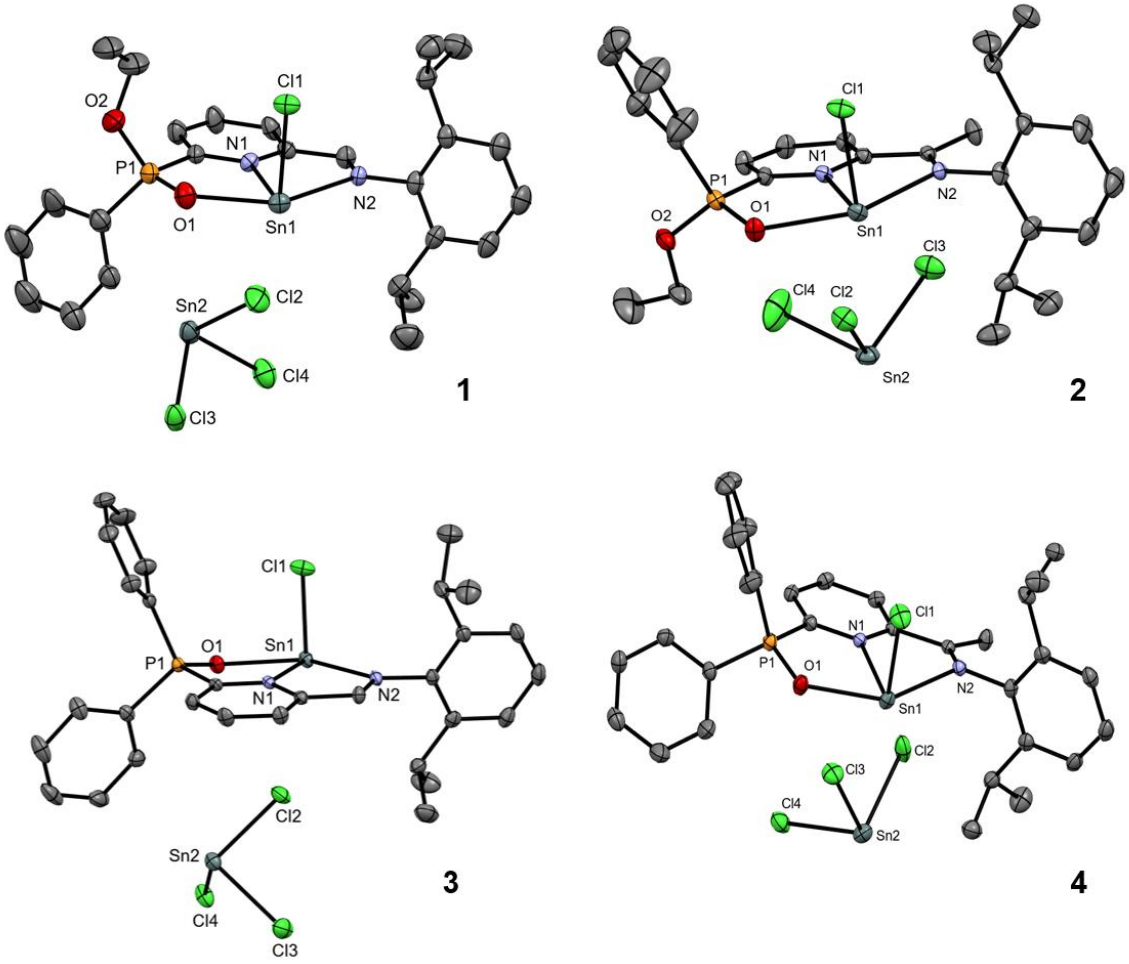

*Figure 4: ORTEP representations of the molecular structures of compounds **1–4**. Hydrogen atoms and CH_2Cl_2 molecules are omitted for clarity.*

In conclusion, in the case of reaction with $SnCl_2$, ligands $\mathbf{L^{3\text{-}6}}$ behave similarly to the related ligands $\mathbf{L^{1\text{-}2}}$ or DIMPY-type ligands[11b,12] and form ionic complexes $[(\mathbf{L^{3\text{-}6}})SnCl]^+[SnCl_3]^-$. The change of groups R^1 (R^1 = H, Me) to the C=N group, or groups R^2 and R^3 ($R^{2,3}$ = Ph, EtO) to the P(O) fragment, does not significantly affect the structures of the resulting compounds. Ligands $\mathbf{L^{3\text{-}6}}$ are coordinated to the central tin atom using two nitrogen and one oxygen atom (κ^3-*N,N,*P(*O*)-coordination).

The possibility of preparation tin(II) dications stabilised by ligands $\mathbf{L^{3\text{-}6}}$ was explored. Equimolar reactions of ligands $\mathbf{L^{3\text{-}6}}$ with $Sn(OTf)_2$ resulted in the formation of tin dications only in the case of ligands $\mathbf{L^4}$ and $\mathbf{L^5}$, leading to the isolation of the corresponding aqua-complexes $[(\mathbf{L^4})Sn(H_2O)][OTf]_2$ (**5**) and $[(\mathbf{L^5})Sn(H_2O)][OTf]_2$ (**6**) as yellow solids (Scheme 4).

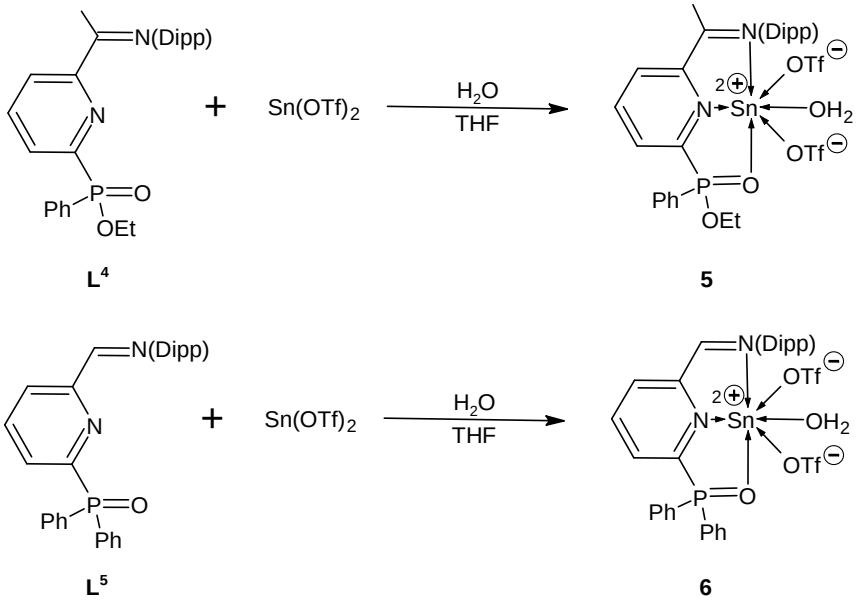

*Scheme 4:Synthesis of tin(II) dications [(**L**⁴)Sn(H₂O)][OTf]₂ (**5**) a [(**L**⁵)Sn(H₂O)][OTf]₂ (**6**).*

The presence of OTf anions in both compounds was confirmed by $^{19}F\{^{1}H\}$ NMR spectroscopy, where signals were observed at δ -79.3 ppm (**5**) a -79.1 ppm (**6**). The IR spectra of both compounds also show broad absorption bands ν = 2960 cm^{-1} (**5**) and 2963 cm^{-1} (**6**), which confirm the presence of the coordinated water molecule.[12]

The stability of the newly prepared compounds **1 - 6** in solution was monitored using $^{31}P\{^{1}H\}$ NMR spectroscopy. It was found that the type of ligand $\mathbf{L^{3-6}}$ and the type of anion are decisive for the stability of the resulting complexes. In the case of the complexes [($\mathbf{L^4}$)Sn(H_2O)][OTf]$_2$ (**5**) and [($\mathbf{L^5}$)Sn(H_2O)][OTf]$_2$ (**6**), where the anionic part is represented by the OTf group, no new signals were detected. The same observation was made for the compounds [($\mathbf{L^5}$)SnCl]$^+$[$SnCl_3$]$^-$ (**3**) and [($\mathbf{L^6}$)SnCl]$^+$[$SnCl_3$]$^-$ (**4**), which have $(Ph)_2PO$ group and the presence of [$SnCl_3$]$^-$ anion in common. Thus, these compounds were found to be stable in the solution even after heating for a prologued time.

On the other hand, in the case of the complexes [($\mathbf{L^3}$)SnCl]$^+$[$SnCl_3$]$^-$ (**1**) and [($\mathbf{L^4}$)SnCl]$^+$[$SnCl_3$]$^-$ (**2**), which have (Ph)(EtO)PO group and the presence of [$SnCl_3$]$^-$ anion in common, new signals were detected in $^{31}P\{^{1}H\}$ NMR at δ 25.6 ppm and 23.7 ppm. These results, combining the absence of any signals for the EtO group in ^{1}H and $^{13}C\{^{1}H\}$ NMR, indicate the cleavage of the Et–O bond and the formation of new corresponding compounds **7** and **8**.

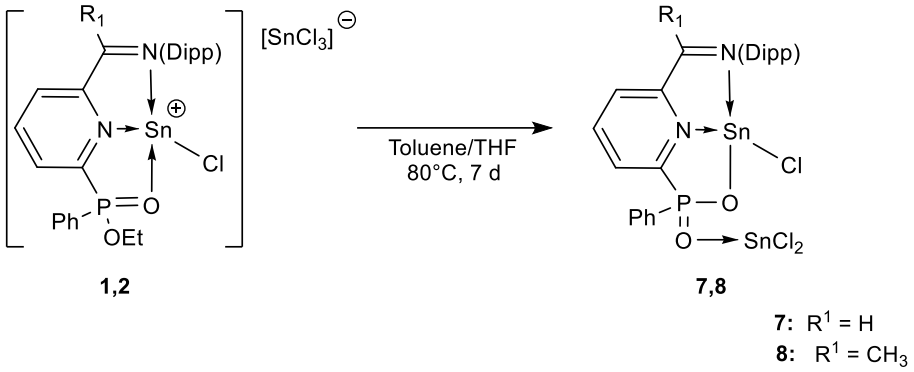

*Scheme 5: Formation of compounds 7 and **8**.*

In $^{119}Sn\{^{1}H\}$ NMR of each compound, two signals were found, showing the presence of two distinct Sn centres (δ -215.8 and -497.4 ppm (**7**), -212.6 and -497.8 ppm (**8**)). We hypothesized that the interaction of the $[SnCl_3]^-$ anion with the Ph(EtO)PO fragment leads to the elimination of EtCl, with the remaining $SnCl_2$ molecule being further coordinated via a P(*O*)→Sn interaction (*δ* -215.8 (**7**), -212.6 (**8**)). This hypothesis was confirmed by single-crystal X-ray diffraction analysis results (Figure 5). The $[SnCl_3]^-$ anion thus acts as a source of the chloride atom, functioning as a nucleophile for the subsequent elimination of EtCl. For this reason, the combination of the $[SnCl_3]^-$ anion with the (RO)P group is a decisive factor for the unstable character of the prepared Sn(II) ions.

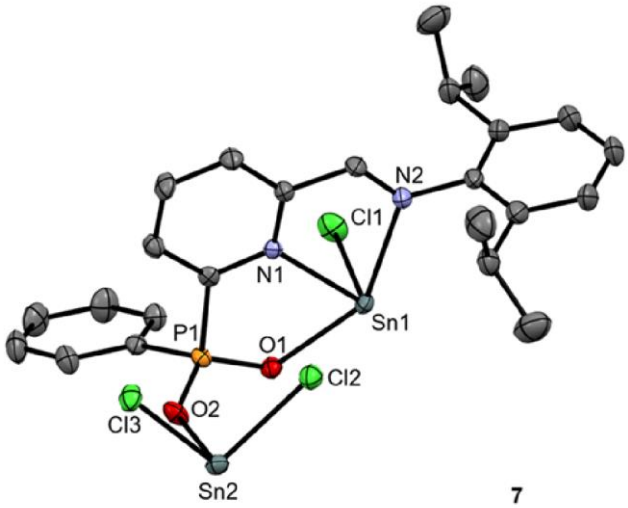

Figure 5: ORTEP representation of the molecular structure of compounds 7.

The bonding situation in compounds **7** and **8** can be described in two different ways. The first possible explanation comes from the ^{119}Sn NMR data, which indicate almost the same chemical shift value for the$[(\mathbf{L}^{3\text{-}6})SnCl]^+$ fragment as compared to the chemical shift value for the complex cations in compounds **1** and **2**. Therefore, complexes **7** and **8** can be described as zwitterionic compounds containing the $[Sn\text{-}Cl]^+$ fragment (Scheme 6A). The positive charge in this case is compensated by the newly formed anion $[O\text{-}SnCl_2]^-$. The negative charge is, in fact, delocalized over the fragment $[O\text{-}P\text{-}O\text{-}SnCl_2]^-$, as indicated by the nearly identical P1–O1 and P1–O2 bond distances.

An alternative explanation for the bonding situation in compounds **7** and **8** is based on the presence of single Sn–O and Sn–Cl bonds and the P=O→$SnCl_2$ interaction (Scheme 6B). The formation of the Sn–O bond leads to the five-membered ring closure, with the closest analogues in the literature being benzoxaphosphastannoles.(13) This explanation is also supported by the chemical shift value observed in the ^{119}Sn NMR for the P=O→$SnCl_2$ (δ = -215.8 ppm (**7**) and δ = -212.6 ppm (**8**)), which is comparable to the chemical shift found for $SnCl_2$·THF (δ = -236 ppm).(14)

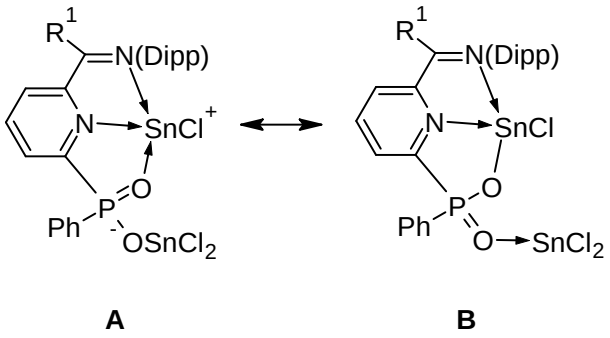

Figure 6: Possible mesomeric forms of 7 and 8: a) zwitterionic explanation, b) single bonds explanation.

1.3 Reactivity of the unsymmetrical N,N,PO-chelating ligand L^2 with non-transition metal chlorides

Given the fact that no significant difference in reactivity was observed between $SnCl_2$ and ligands L^{3-6} compared to ligands $L^{1,2}$, further investigation of the reactivity of these N,N,PO-chelating ligands was limited to ligand L^2 for practical reasons such as solubility, facile preparation, and reaction yields.

The study of the reactivity of ligand L^2 was focused on reactions with selected Lewis acids of the non-transition elements, namely $GeCl_2$·dioxane, Ph_3SnCl, Ph_2SnCl_2, $SeCl_4$, and $TeCl_4$. Reaction of ligand L^2 with Gethe Cl_2·dioxane led to the formation of the complex [(L^2)GeCl][$GeCl_3$] (**9**) (Scheme 6). NMR data for compound **9** match the data reported in the literature.(12)

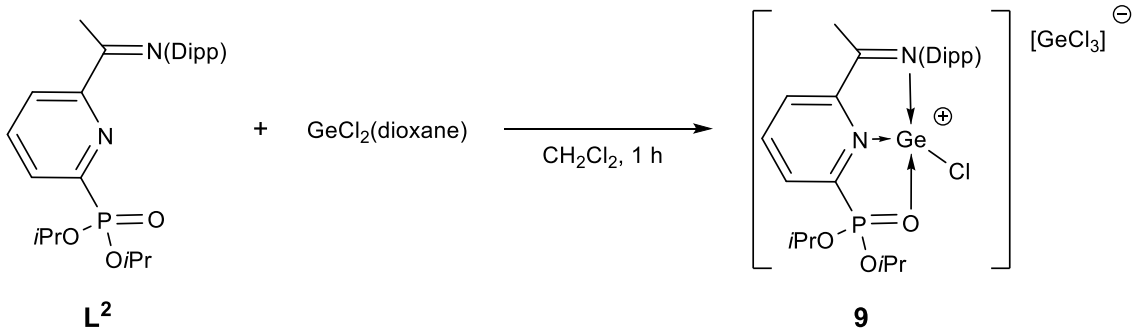

*Scheme 6: Synthesis of germanium(II) complex **9**.*

Based on these findings, it is evident that in the case of reactions of ligand L^2 with ECl_2 (E = Sn, Ge), the formation of ionic complexes of the type [(L^2)ECl]$^+$[ECl_3]$^-$ occurs, and ligand L^2 shows a tendency towards κ^3-*N,N*,P*(O)*-coordination. In contrast,

reactions of ligand **L²** with Ph_3SnCl or Ph_2SnCl_2 led to the formation of neutral complexes [(**L²**)$SnPh_3Cl$] (**10**) and [(**L²**)$SnPh_2Cl_2$] (**11**) (Scheme 7).

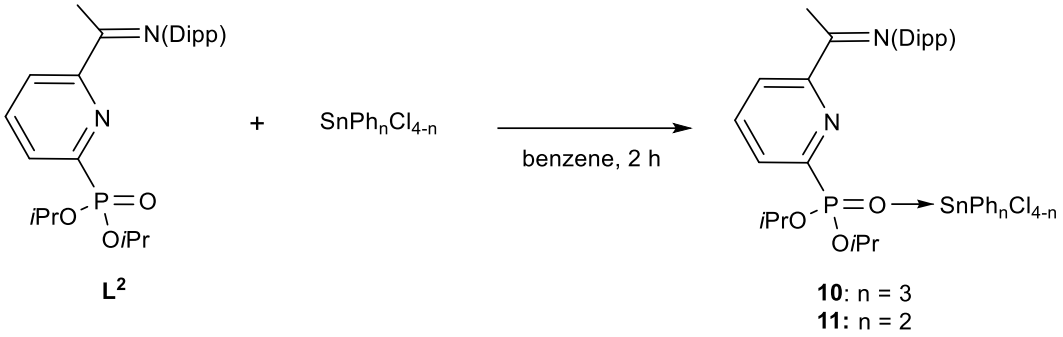

*Scheme 7: Synthesis of tin(IV) complexes with $SnPh_nCl_{4-n}$ (**10:** n = 3; **11:** n = 2).*

NMR data revealed only a presence of weak interaction occurring between the $(i\text{PrO})_2\text{P=O}$ group of ligand **L²**. There is no significant shielding at the P atom, and there is no indication of nitrogen atoms from ligand **L²** involvement in interaction with the starting compounds Ph_3SnCl or Ph_2SnCl_2. This aligns with the results of X-ray diffraction analysis, which unambiguously established the existence of the neutral complexes [(**L²**)$SnPh_3Cl$] (**10**) and [(**L²**)$SnPh_2Cl_2$] (**11**) (Figure 7).

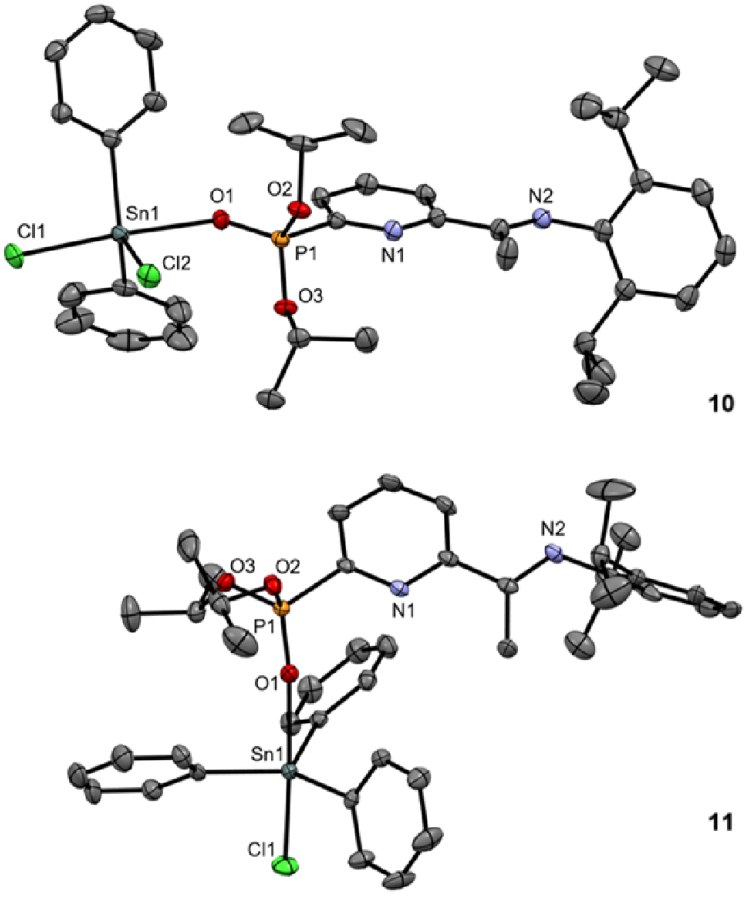

*Figure 7: ORTEP representation of the molecular structure of compounds **10** and **11**.*

Based on the results above, it is evident that the ligand **L²** behaves as a κ¹-*O*-chelating ligand in reactions with Ph_3SnCl or Ph_2SnCl_2, which significantly differs from its previously described κ³-*N,N,*P(*O*)-coordinating motif in Sn(II) and Ge(II) ionic compounds. Furthermore, the reactions of ligand **L²** with halides of group 15 and 16 heavier elements were also studied. While reactions of **L²** with $BiCl_3$ and $SbCl_3$ did not yield characterisable products, the reaction of **L²** with $SeCl_4$ a $TeCl_4$ proceeded via activation of the C-H bond in the methyl group (C*H*₃)C=N. Both reactions were initially monitored using $^{31}P\{^1H\}$ NMR spectroscopy, and new signals were found at *δ* 4.7 ppm (for reaction with $SeCl_4$) and δ 5.0 ppm (for reaction with $TeCl_4$). New compounds **12** and **13**, containing corresponding newly formed CH=$SeCl_2$ (**12**, Scheme 8A) and CH_2-$TeCl_3$ (**13**, Scheme 8B) bonds, were subsequently isolated from these reactions.

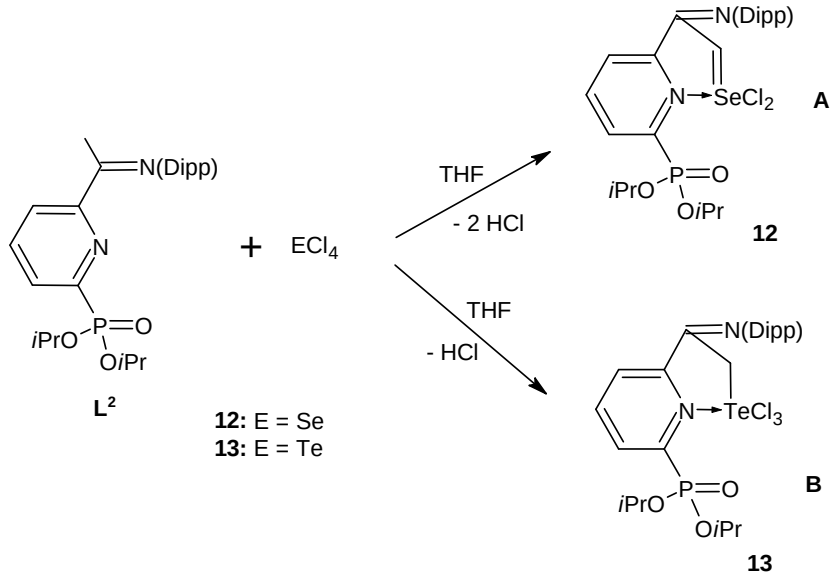

*Scheme 8: Synthesis of group 16 complexes **12** (Se) and **13** (Te).*

The ^1H NMR spectra of compounds **12** and **13** revealed the absence of the methyl (C*H*₃)C=N group signal (around *δ* ~ 2.3 ppm). Instead, a new signal was observed at *δ* 6.08 ppm, with an integral intensity of 1. This chemical shift and integral intensity correspond to the presence of a methine (=C*H*)C=N group in compound **12**. In contrast, in the spectrum of compound **13**, a new signal was found at *δ* 4.22 ppm, with an integral intensity of 2, defining the presence of a methylene (-C*H*₂)C=N group in compound **13**. These findings were further solidified by the results from $^{13}C\{^1H\}$ NMR and ^1H-^{13}C HSQC NMR spectroscopy. Due to the presence of interaction constants $^1J(^{77}Se, ^{13}C)$ and $^1J(^{125}Te, ^{13}C)$ in $^{13}C\{^1H\}$ NMR, we hypothesised that in compound **12**, the Se atom is directly connected to the (=*CH*)C=N fragment, thus forming the (Se=*CH*)C=N motif, and in compound **13**, the Te atom is directly connected to the (-*CH*₂)C=N fragment, hence defining the (Te-*CH*₂)C=N motif. It was later confirmed by MS-MALDI TOF results, where the m/z = 557.12 signal in MS^+ was assigned to the [**12**-Cl]$^+$ fragment. The structure of compound **13** was confirmed using single-crystal X-ray diffraction analysis (Figure 8).

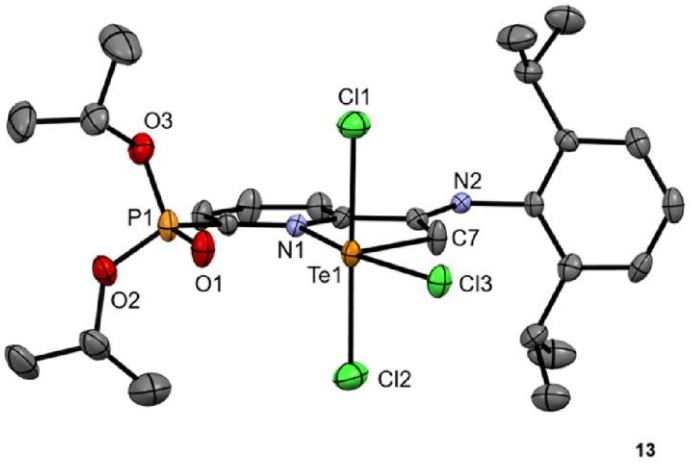

*Figure 8: ORTEP representation of the molecular structure of compound **13**.*

Therefore, ligand $\mathbf{L^2}$ can form complexes with various coordination motifs when reacting with different halides of non-transition elements. In the case of the ionic complexes $[(\mathbf{L^2})SnCl]^+[SnCl_3]^-$ a $[(\mathbf{L^2})GeCl]^+[GeCl_3]^-$ (**9**), all donor atoms of ligand $\mathbf{L^2}$ are involved in coordination, resulting in a κ^3-*N,N,*P(*O*)-chelating motif in these compounds. In some instances, only the oxygen atom of ligand $\mathbf{L^2}$ participates in coordination, leading to a κ^1-*O*-coordination type (compounds **10** and **11**). Lastly, κ^2-*C,N*-coordination of ligand $\mathbf{L^2}$ was also observed in compounds **12** and **13** as a result of C-H bond activation.

1.4 Reactivity of complex 9

The diversity of coordination motifs in ligands $\mathbf{L^{2\text{-}6}}$ and the presence of the E-Cl bond in the prepared complexes **1 – 13** opens the possibility for reduction reactions. Unfortunately, reactions of all prepared compounds **1 - 13** with reducing agents such as Na, K, KC_8 or $Li[BEt_3H]$ led to the elimination of an insoluble metal precipitate and the release of free ligands into the solution. The only successful reduction was observed in the reaction of the compound $[(\mathbf{L^2})GeCl]^+[GeCl_3]^-$ (**9**) with an excess of K in benzene, where a colour change from yellow to intense red was evident by the naked eye. The isolated red complex $[(\mathbf{L^2})Ge]$ (**14**) (Scheme 9) is extremely sensitive to moisture and air.

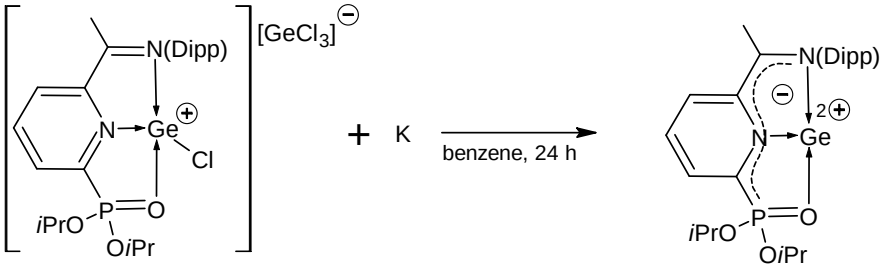

*Scheme 9: Reduction of complex **9** resulting in the formation of compound **14**.*

Compound **14** can be described as a complex with a Ge atom in the +II oxidation state, and therefore, the structure of the originally neutral ligand $\mathbf{L^2}$ accepts two

electrons, resulting in the formation of the anionic form $(\mathbf{L^2})^{2-}$. This claim was later supported by the results of single-crystal X-ray diffraction analysis (Figure 9).

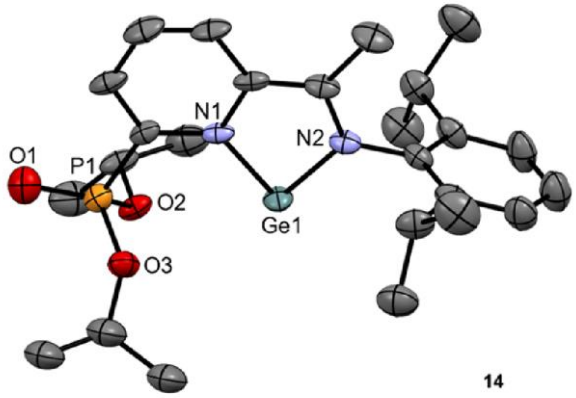

*Figure 9: ORTEP representation of the molecular structure of compound **14**.*

Additionally, complex $[(\mathbf{L^2})GeCl]^+[GeCl_3]^-$ (**9**) was also found to be a suitable precursor for the preparation of GeTe nanoparticles during the studies aimed to improve the stability of L^2-based complexes. Compound **9** can undergo a substitution reaction with Ag(OTf), leading to the formation of the ionic complex $[(\mathbf{L^2})GeCl]^+[OTf]^-$ (**15**) (Scheme 10).

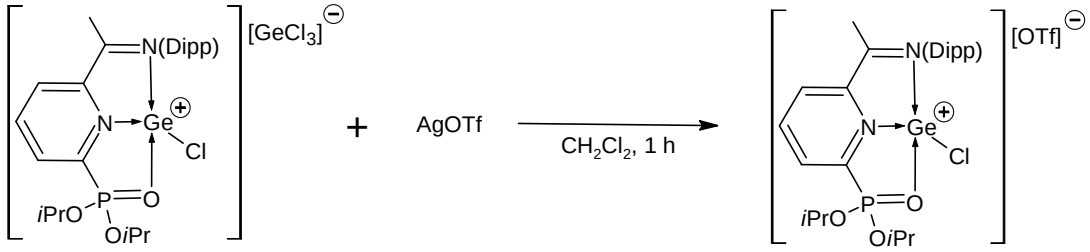

*Scheme 10: Synthesis of compound **15**.*

Analogically to complexes **1-6**, the stability of complex **15** was studied in a toluene solution, where no new signal indicating the decomposition of the original complex **15** was observed in the $^{31}P\{^1H\}$ NMR. Therefore, this complex $[(\mathbf{L^2})GeCl]^+[OTf]^-$ (**15**) was further tested in substitution reactions. In the reaction of **15** with Li_2Te, an insoluble solid was formed, while the presence of free ligand $\mathbf{L^2}$ was detected in the THF solution in the $^{31}P\{^1H\}$ NMR (Scheme 11). The solid residue was washed and subsequently characterised by Raman spectroscopy as GeTe material.

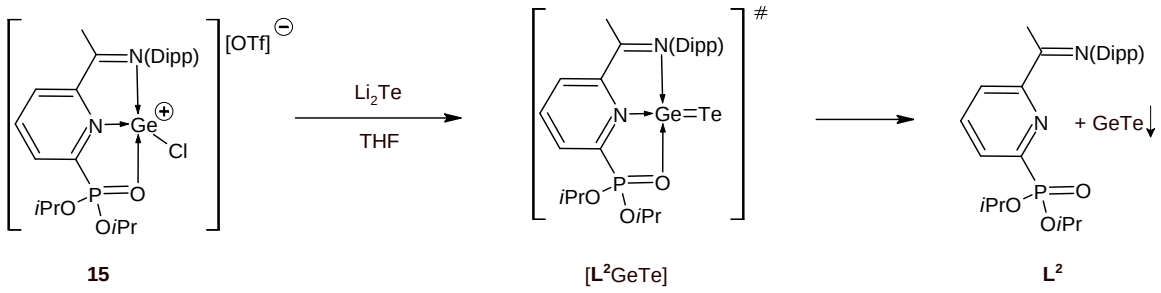

*Scheme 11: Application of complex **15** for the preparation of GeTe nanoparticles.*

Complex **15** was, therefore, further investigated as a potential precursor for the formation of GeTe nanoparticles from solution at room temperature (RT). During the initial testing, the reaction was carried out at RT for 24 hours. The obtained black powder was characterised by dynamic light scattering (DLS). The histogram of the hydrodynamic diameter (D_H) contained signals of primary particles and their agglomerates (bimodal). The hydrodynamic diameter of the primary particles (D_H = 60 nm) increased due to agglomeration to D_H = 700 nm (with an average ΔD_H = 550 nm) (Figure 10, black curve).

The reaction conditions needed to be improved, and for this purpose, the influence of sonication was further tested. Similar to the previous method Li_2Te in THF was added to the solution of complex **15** at RT and additionally sonicated for 10 minutes at RT. DLS analysis revealed a bimodal distribution of the particle population (Figure 10, blue curve), with a hydrodynamic diameter of the primary particles (D_H = 115 nm), while the hydrodynamic size of the agglomerates decreased to D_H = 255 nm. From these results, it is evident that the use of sonication had a negative impact on increasing the primary particle population, and this method also does not lead to the formation of GeTe nanoparticles that, from the definition, require D_H under 100 nm.

Subsequently, the effect of low temperature was studied. Compared to the pervious methods, the reaction temperature was lowered to -50 °C. The hydrodynamic diameter of the primary particles obtained in this way decreased to D_H = 71 nm (Figure 10, red curve). Based on these findings, the proposed mechanism for the formation of GeTe particles includes an unstable complex [(**L**^{2})GeTe] formation in the first phase of the reaction of **15** s Li_2Te. Due to thermal instability, even at temperatures below -50 °C, the intermediate then decomposes into primary GeTe particles of varying sizes (Scheme 11). Thus, lowering the temperature from RT to -50 °C slows down this process, allowing the formation of smaller particles, but we were not able to fully stabilize complex [(**L**^{2})GeTe] for long enough to perform characterisation of the intermediate.

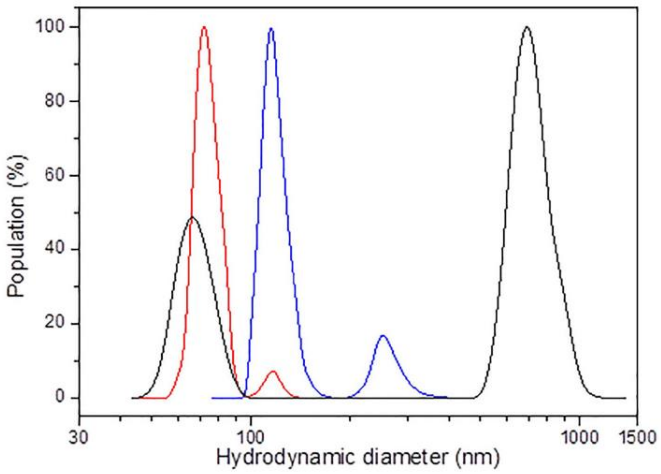

Figure 10: Histograms of the hydrodynamic diameter for GeTe particles: synthesis at RT (black); synthesis at RT with sonication (blue); synthesis at -50 °C (red).

The low-temperature procedure was then optimised and repeated, and the resulting powder was subsequently used for further characterisation. In the powder XRD two very broad halos and no sharp diffraction peaks were observed, indicating the amorphous nature of the material. Morphological analysis using TEM/BF confirmed the isometric shape of nanoparticles without characteristic crystal facets, with an average particle size of nearing 20 nm. The SEM EDX measurements established a composition of $Ge_{48}Te_{52}$ (±2 at.%), with a homogeneous distribution of Ge and Te elements in the whole sample.

In the follow-up study on the influence of concentration on particle size and agglomeration, two representative concentrations of GeTe in THF were selected for comparison (5 mg/ml and 0.5 mg/ml). It was found that at a concentration of 5 mg/ml, GeTe mainly formed agglomerates (Figure 11a). However, even within these agglomerates, particles with a size of approximately 136 nm could still be identified. Reducing the concentration to 0.5 mg/ml led to the formation of well-separated GeTe particles with a size ca 155 nm (Figure 11b).

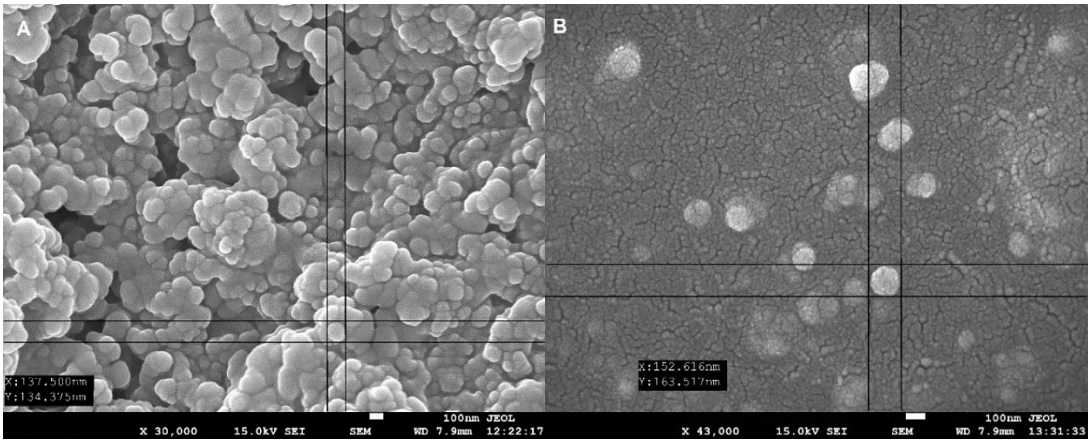

Figure 11: a) HR-SEM image of GeTe particles (suspension 5 mg/ml); b) HR-SEM image of GeTe particles (suspension 0.5 mg/ml).

For comparison of the temperature effect on the resulting particle structure, samples prepared at room temperature and at -50 °C were selected for Raman spectroscopic analysis. The recorded spectra were almost identical, indicating the fact that the temperature affects only the size of agglomerates but not the structure of the particles. The most intensive bands in the Raman spectrum were assigned to vibrations in bending mode (90 cm^{-1}), symmetric stretching modes (120 and 159 cm^{-1}), and antisymmetric stretching mode (221 cm^{-1}) of the $GeTe_{4-n}Ge_n$ tetrahedra. A band with lower intensity (370 cm^{-1}) was attributed to the presence of a homopolar bond with the population between 6-10% in the GeTe structure.[14] In the LA TOF of GeTe nanoparticles were detected Te_n^- (n = 1-5), $GeTe_n^-$ (n = 2-4) and $Ge_mTe_n^-$ (m = 2-6, n = 1-3) clusters.

It can thus be concluded that the preparation of stable complex $[(\mathbf{L^2})GeCl]^+[OTf]^-$ (**15**) unlocked a reliable pathway for the formation of well-defined GeTe nanoparticles that can be further used with various substrates due to the great solubility of the starting material under described conditions.

1.5 Application of Sn(II) ions in the ROP of cyclic esters

In our group, N,N-coordinated Sn(II) cations **16–18** (Figure 12) were previously prepared and used as catalysts for the ring-opening polymerisation (ROP) of L-lactide (L-LA).[15,17] Analogous *N,N*,P(*O*)-coordinated Sn(II) cations **2, 6,** and **8** were also tested as an attempt to increase a library of catalysts for the ROP of L-lactide.

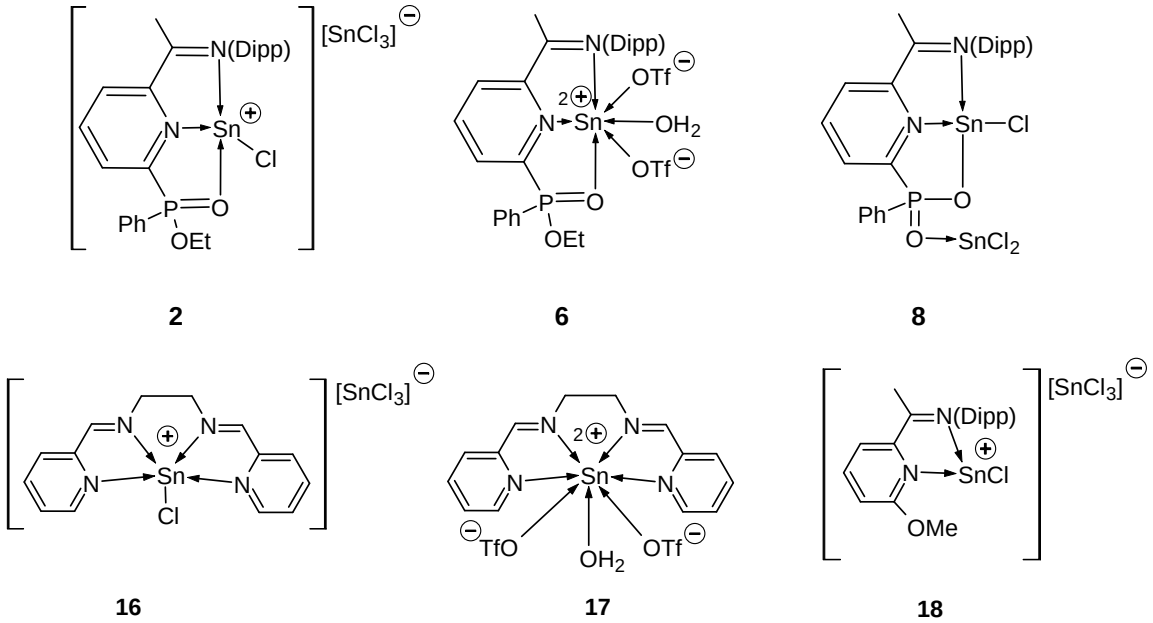

2 **6** **8**

16 **17** **18**

Figure 12: Selected N-coordinated tin cations for catalytic reactivity testing in ROP.

The conditions for the ROP of L-LA were analogues to the established catalysts **16-18**,[15,17] where Sn(II) complexes, along with benzyl alcohol (BzOH) and L-LA, were placed in a reaction flask with a loading molar ratio of [L-LA]:cat:BzOH = 100:1:1. All reactions were carried in melted L-LA previously homogenised with the rest of the

mixture to avoid data fluctuations at 145°C. The conversions were determined from the results of ^{1}H NMR spectroscopy.

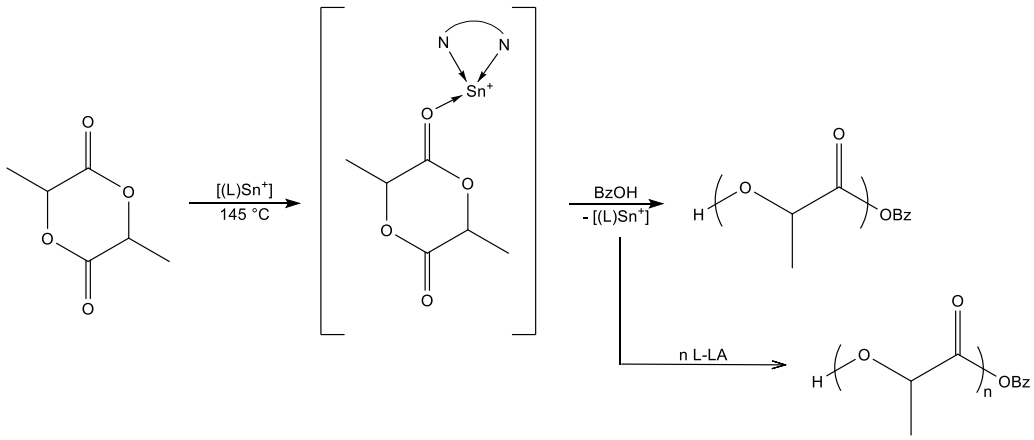

Scheme 12: ROP of L-LA catalysed by Sn(II) complexes.

Unfortunately, all new complexes **2**, **6**, and **8** exhibited very low catalytic activity with conversions below 20%. As a result, only the representative N,N-coordinated Sn(II) compounds **16-18** were regarded as suitable for further catalytic studies.

These compounds demonstrated good control over the polymerisation of L-LA during previous studies.[15] Therefore, we proposed that the characteristics of catalysts **16-18** could be applied to the synthesis of star-shaped PLAs. Conditions similar to the preparation of linear PLAs were used. Catalysts **16-18** and [L-LA] were placed in a reaction flask in a molar ratio of [L-LA]:cat = 100:1. However, different polyalcohols (n(OH) = 3-6) were used as initiators, and to ensure equal catalytic conditions for all experiments, the molar ratio was set to cat:[OH] = 1:1. For example, in a model reaction dipentaerythritol (DPE) (n(OH) = 6) was used as the initiator. Thus, the molar ratio was set to [L-LA]:cat:[DPE] = 100:1:1/6 (Scheme 13). The isolated polymers **PLA-DPE 1**, **PLA-DPE 2**, and **PLA-DPE 3** showed quantitative conversions similar to the results for the linear PLAs under the same conditions.

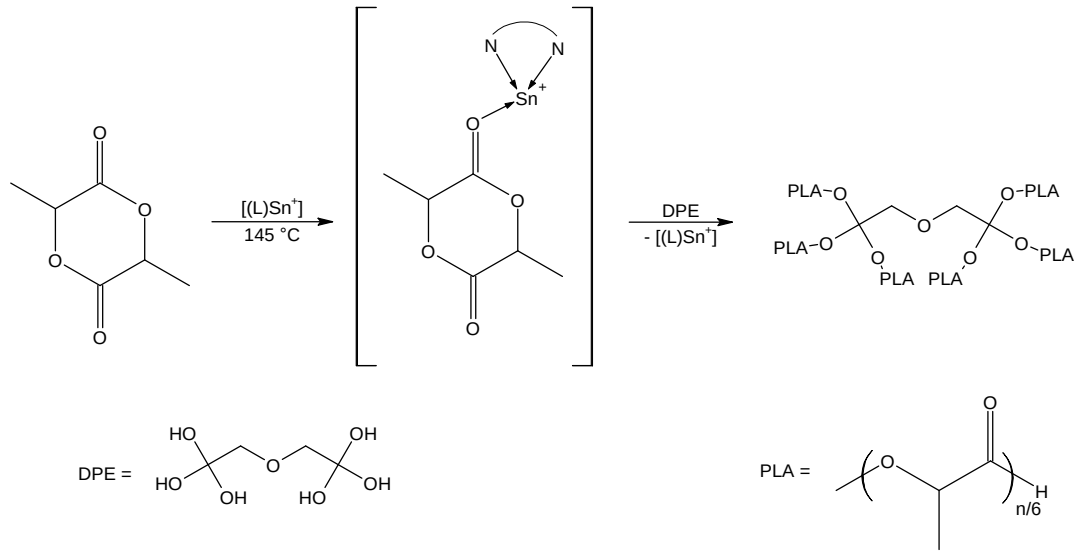

*Scheme 13: Synthesis of star-shaped PLA-DPE using complexes **16-18** as catalysts.*

The weight-average intrinsic viscosity values ($[\eta]_w$) of the **PLA-DPE 1** and **PLA-DPE 2** polyesters are significantly lower than those of the linear PLA, which suggests the presence of a branched structure. In contrast, this difference for the **PLA-DPE 3** polyester is less pronounced, indicating a lower number of arms (Figure 13).

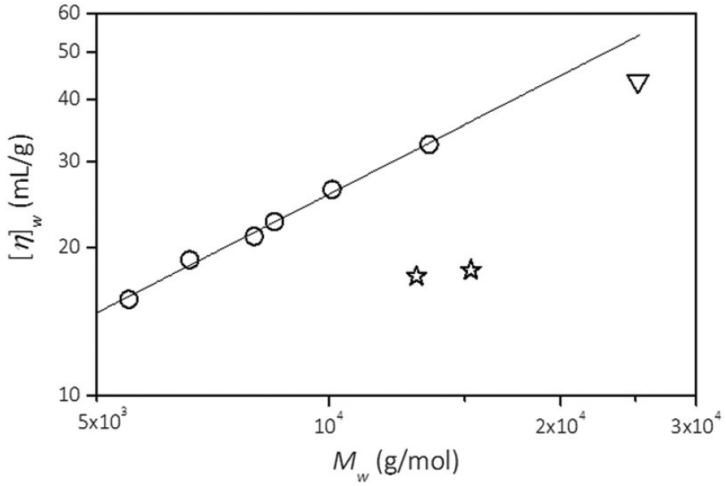

*Figure 13: The plots with the y-axis $[\eta]_w$ versus the x-axis M_w for linear PLA (○), samples **PLA-DPE 1**, **PLA-DPE 2** (☆) and **PLA-DPE 3** (▽).*

The molar mass distribution and branching of the resulting PLAs were characterised using size exclusion chromatography (SEC) with a multi-angle light scattering (MALS) detector and an online viscometer (Visco). The information about number-average molar mass (M_n), weight-average molar mass (M_w), dispersity (M_w/M_n), and weight-average intrinsic viscosity ($[\eta]_w$) of the **PLA-DPE 1**, **PLA-DPE 2**, and **PLA-DPE 3** samples is presented in Table 1.

Table 1: ROP of star-shaped PLA based on DPE as the initiator.

Sample	Catalyst	M_n [g/mol]	M_w [g/mol]	Đ	$[\eta]_w$ [ml/g]	f
PLA-DPE 1	**16**	13200	15300	1,15	18.0	7.2
PLA-DPE 2	**17**	8500	13000	1,53	17.5	6.1
PLA-DPE 3	**18**	12400	25200	2,03	43.7	3.2

The average number of arms can be estimated using the branching ratio $g'(M_w)$,[18] where the subscripts $[\eta]_{branched}$ and $[\eta]_{linear}$ refer to branched and linear polymers with the same weight-average molar mass (M_w):

$$g'(M_w) = \left(\frac{[\eta]_{rozvětvený}}{[\eta]_{lineární}}\right)_{M_w}$$

The number of arms f, can then be calculated from the branching ratio using the equation: [19]

$$g' = \left[\left(\frac{3f-2}{f^2}\right)^{0.58}\right]\left[\frac{0.724 - 0.015(f-1)}{0.724}\right]$$

To calculate the branching ratio $g'(M_w)$, the Mark-Houwink constant obtained from the Mark-Houwink plots of linear PLAs is required:

$$[\eta] = 0.0158 \times M^{0.803} \text{ (THF, 25 °C)}$$

The values of f indicate a good agreement between the experimental and theoretical number of arms for catalysts **16** (f = 7.2) and **17** (f = 6.1), while for catalyst **18**, the calculations suggest a lower number of arms compared to the theory (f = 3.2). Therefore, for further experiments with polyalcohols, only complexes **16** and **17** were used.

The data summarised in Table 2 indicates no significant effect of the catalyst on the dispersity (Đ), which remains relatively constant for all obtained star-shaped polyesters ***PLA1-14** (Đ = 1.09 - 1.91). The lowest dispersity (Đ = 1.09) was observed in the case of a catalytic system containing compound **17** as the catalyst and glycerol as the polymerisation initiator (***PLA8**). On the other hand, the combination of complex **16** with xylitol (***PLA5**) provided a polymer with the highest dispersity (Đ = 1.91).

A certain influence of the catalyst is observed in the case of the number-average molar mass (M_n) parameter, where the experimental $M_{n,SEC}$ for PLAs catalysed by compound **16** reach approx. half of the theoretical $M_{n,t}$. On the other hand, the application of catalyst **17** led to experimental $M_{n,SEC}$ values were in agreement with $M_{n,t}$ values, particularly for such initiators as triethanolamine (***PLA10**), xylitol (***PLA12**), and D-sorbitol (***PLA14**). These results suggest better control over the polymerisation process for catalyst **17** in the synthesis of star-shaped polylactides.

Overall, the number of arms f for ***PLA1-14** ranged from 2.3 to 5.2 (n(OH) = 3-6), indicating that the experimental number of arms is always somewhat lower than the theoretical value. The values for ***PLA8-14** (f = 2.6 to 5.2) approach the theoretical

number of arms (except for ***PLA13**), thus confirming better control over the ROP process when catalyst **17** is used in star-shaped PLAs preparation.

Table 2: ROP of star-shaped PLAs using various polyalcohols as initiators.

***PLA**	**Cat.**	**Initiator**	**Conv. [%]**	**$M_{n,t}$ [g/mol]**	**$M_{n,SEC}$ [g/mol]**	***Đ***	***f***
1	**16**	glycerol	96	13900	6000	1.27	2.3 (3)
2	**16**	trimethylolpropane	85	12300	5700	1.16	2.5 (3)
3	**16**	triethanolamine	96	13900	6300	1.19	2.6 (3)
4	**16**	pentaerythritol	96	13900	9000	1.70	3.1 (4)
5	**16**	xylitol	97	14000	7700	1.91	3.7 (5)
6	**16**	*myo*-inositol	88	12700	10100	1.51	2.7 (6)
7	**16**	D-sorbitol	96	13900	8200	1.80	4.1 (6)
8	**17**	glycerol	95	13700	6800	1.09	2.6 (3)
9	**17**	trimethylolpropane	89	12800	9600	1.22	2.7 (3)
10	**17**	triethanolamine	94	13600	12200	1.14	3.8 (3)
11	**17**	pentaerythritol	97	14000	11900	1.45	3.6 (4)
12	**17**	xylitol	97	14000	13200	1.32	4.4 (5)
13	**17**	*myo*-inositol	85	12300	8500	1.22	4.1 (6)
14	**17**	D-sorbitol	94	13600	12700	1.57	5.2 (6)

In conclusion, the iminopyridine scaffold is a highly promising system for the synthesis of Sn(II) cations with strong Lewis acidity. The nature of the substituents in the *ortho*-positions of the iminopyridine-based ligands influences the Lewis acidity of these cations. Certain N,N-coordinated Sn(II) cations (**16-18**) exhibit consistent catalytic activity in the ROP of L-lactide, allowing for the preparation of both linear and star-shaped polylactides.

For this reason, N-coordinated gallium boroxines containing multiple hydroxyl groups were prepared and tested as potential polyalcohol initiators for the synthesis of star-shaped polylactides. However, these compounds did not have a promising conversion rate, and star-shaped PLAs incorporating these gallium boroxines have yet to be obtained.

4. Conclusion

This dissertation, built upon previous studies conducted throughout the years in prof. Jambor's group, contributes to the synthesis and characterisation of tin complexes based on iminopyridine ligands. New asymmetric ligands (**L$^{3-6}$**) were synthesised and tested in reactions with $SnCl_2$. The formed auto-ionized complexes [(**L$^{3-6}$**)SnCl]$^+$[SnCl3]$^-$ (**1-4**) are similar to previously studied complexes **16-18**, showcasing consistent ligand behaviour in the presence of $SnCl_2$. Amongst others, these complexes were tested for stability in solution, and for complexes **1** and **2**, both containing the (Ph)(EtO)PO fragment, the absence of EtO group signals in ^{1}H NMR, along with the results of single-crystal X-ray analysis, indicates the cleavage of the Et–O bond and the formation of new compounds **7** and **8**. Opposite to that, prepared tin(II) dications **6** and **7** were stable regardless of the R^2 and R^3 groups on the P(O) fragment.

The coordination versatility of this ligand system on the example of ligand **L^2** was explored in reactions with non-transition element salts. Notably, reaction with $GeCl_2$ formed a κ^3-*N,N,*P*(O)*-coordinated complex [(**L^2**)GeCl]$^+$[$GeCl_3$]$^-$ (**9**), while reactions with Ph_3SnCl and Ph_2SnCl_2 produced corresponding κ^1-*O*-coordinated complexes **10** and **11**. Furthermore, reactions with $TeCl_4$ and $SeCl_4$ led to the formation of corresponding κ^2-*C,N*-coordinated complexes **12** and **13**.

Reduction reactions were also studied, although they mostly led to ligand release and the formation of insoluble precipitates. However, a successful reduction reaction with the [(**L^2**)GeCl]$^+$[$GeCl_3$]$^-$ complex (**9**) resulted in the formation of the [(**L^2**)Ge] complex (**14**), containing anionic ligand (**L^2**)$^{2-}$, demonstrating the non-innocent behaviour of the ligand.

In terms of applications, the low-temperature synthesis of GeTe nanoparticles using [(**L^2**)GeCl]$^+$[OTf]$^-$ (**15**) as a precursor was successfully developed. These GeTe nanoparticles were then characterised, and the influence of various factors on the particle size and agglomeration was studied.

In an area of catalysis, the novel *N,N,*P(*O)*-coordinated tin complexes (**2**, **6**, **8**) showed poor activity in the ROP of L-LA, with conversions under 20%. However, more catalytically active Sn(II) complexes **16-18** were successfully used in the synthesis of star-shaped PLAs with different numbers of arms (n = 3-6).

5. List of references

1) V. Nesterov, D. Reiter, P. Bag, P. Frisch, R. Holzner, A. Porzelt, S. Inoue, *Chem. Rev.,* **2018**, 118 (19), 9678-9842.
2) M. M. Watt, M. S. Collins, D. W. Johnson, *Acc. Chem. Res.,* **2013**, 46 (4), 955-966.
3) C. Bakewell, A. J. P. White, M. R. Crimmin, *Chem. Sci.*, **2019**, 10, 2452.
4) X. Wu, M. Tamm, *Coord. Chem. Rev.*, **2014**, 260, 116-138.
5) L. Bourget-Merle, M. F. Lappert, J. R. Severn, *Chem. Rev.*, **2002**, 102, 3031−3065.
6) a) M. Gasperini, F. Ragaini, S. Cenini, *Organometallics*, **2002**, 21 (14), 2950-2957; b) E. C. Alyea, P. H. Merrell, *Synth. React. Inorg. Met. Org. Chem*., **1974**, 4(6), 535-544.
7) S. K. Ibrahim, A. V. Khvostov, M. F. Lappert, L. Maron, L. Perrin, C. J. Pickett, A. V. Protchenko, *Dalton Trans*., **2006**, 35, 2591–2596.
8) T. Smit, A. K. Tomov, V. C. Gibson, A. J. P. White, D. Williams, *J. Inorg. Chem*., **2004**, 43, 6511.
9) M. Pramanik, M. G. Guerzoni, E. Richards, R. L. Melen, *Chem. Int. Ed*., **2024**, 63, e202316461.
10) a) J. L. Dutton, G. J. Farrar, M. J. Sgro, T. L. Battista, P. J. Ragogna, *Chem. Eur. J*., **2009**, 15, 10263; b) J. Flock, B. Steller, P. Unger, B. Gerke, R. Pöttgen, R. Fischer, *Zeitschrift für Naturforschung B*, **2017**, 72(11), 883-894.
11) a) H. A Jenkins, C/ L Dumaresque, D. Vidovic, J. AC. Clyburne, *Can. J. Chem*., **2002**, 80 (11), 1398-1403; b) M. Bouska, L. Dostal, A. Ruzicka, R. Jambor, *Organometallics*, **2013**, 32, 1995.
12) M. Syková. Neutral N,N,O-chelating ligands in chemistry of 14th group elements. Master's thesis. University of Pardubice, Faculty of Chemical Technology, Department of General and Inorganic Chemistry. Supervisor Prof. Ing. Roman Jambor, Ph.D., Pardubice, **2021**.
13) M. Mehring, I. Vrasidas, D. Horn, M. Schürmann, K. Jurkschat, *Organometallics*, **2001**, 20, 4647.
14) P. Pyykkö, M. Atsumi, *Chem. Eur. J.,* **2009**, 15,12770.
15) T. Panchartková. N→M coordinating cations of group 14th elements: Synthesis and reactivity. Master's thesis. University of Pardubice, Faculty of Chemical Technology, Department of General and Inorganic Chemistry. Supervisor Prof. Ing. Roman Jambor, Ph.D., Pardubice, **2020**.
16) W. Lan, L. Cao, Y. Fu, J. Fang, J. Zhang, J. Wang. *Vacuum,* **2022**, 197, 110847.
17) M. Bouška, L. Dostál, A. Růžička, R. Jambor, *Organometallics*, **2013**, 32(6), 1995–1999.
18) S. Podzimek, Light Scattering, Size Exclusion Chromatography and Asymmetric Flow Field Flow Fractionation: Powerful Tools for the Characterization of Polymers, Proteins and Nanoparticles, *Wiley*, **2011**, ISBN: 9780470877975.
19) J. Douglas, J. Roovers, K. Freed, *Macromolecules*, **1990**, 23, 4168.

6. List of Students' Published Works

1) M. Bouška, **Y. Milasheuskaya**, M. Šlouf, P. Knotek, S. Pechev, L. Prokeš, L. Pečinka, J. Havel, M. Novák, R. Jambor, P. Němec. LOW-TEMPERATURE SYNTHESIS OF GeTe NANOPARTICLES. *Chem. - Eur. J.,* **2024**, e202402319. DOI: 10.1002/chem.202402319
2) M. Novák, **Y. Milasheuskaya**, M. Srb, S. Podzimek, M. Bouška, R. Jambor. Synthesis of star-shaped poly(lactide)s, poly(valerolactone)s and poly(caprolactone)s via ROP catalysed by N-donor tin(ii) cations and comparison of their wetting properties with linear analogues. *RSC Adv.*, **2024**, 14, 23273-23285. DOI: 10.1039/d4ra03515a
3) M. Novák, J. Turek, **Y. Milasheuskaya**, M. Syková, M. Dostal, J. Stalmans, Z. Růžičková, K. Jurkschat, R. Jambor. Tin(II) cations stabilised by non-symmetric N, N',O-chelating ligands: synthesis and stability. *Dalton Trans.*, **2023**, 52, 2749-2761. DOI:10.1039/d2dt03563d
4) M. Novák, J. Turek, **Y. Milasheuskaya**, Z. Růžičková, S. Podzimek, R. Jambor. N-Donor stabilised tin(II) cations as efficient ROP catalysts for synthesising linear and star-shaped PLAs via the activated monomer mechanism. *Dalton Trans.*, **2021**, 50, 16039-16052. DOI: 10.1039/d1dt02658e
5) **Y. Milasheuskaya,** J. Schwarz, L. Dostal, Z. Růžičková, M. Bouška, Z. Olmrová Zmrhalová, T. Syrový, R. Jambor. Synthesis and optical properties of N→Ga coordinated gallium boroxines. *Dalton Trans.,* **2021**, 50, 18164-18172. DOI: 10.1039/d1dt02975d
6) M. Srb, **Y. Milasheuskaya**, R. Jambor, K. Kopecká, P. Knotek. Low-Temperature Sn0 Nanoparticles Synthesis by Means of Tin(II) N,N-Complexes Reduction. *ChemistrySelect,* **2021**, 6, 3926-3931. DOI: 10.1002/slct.202100618